

The method of the fundamental solutions and its modifications for electromagnetic field problems

C. S. Chen

*Department of Mathematics
University of Southern Mississippi
Hattiesburg, MS 39406, USA*

S. Y. Reutskiy, V. Y. Rozov

*Science and Technology Center of Magnetism of Technical Objects
The National Academy of Science of Ukraine
19 Industrialnaya St., 61106, Kharkov, Ukraine*

(Received in the final form January 14, 2009)

The paper presents the method of fundamental solutions (MFS) for solving electromagnetic problems. We compare the MFS with the method of boundary integral equations in solution of potential problems. We demonstrate the MFS technique together with the Laplace transform in application to the problem of scattering of electromagnetic pulses. A modification of the MFS - the method of approximate fundamental solutions (MAFS) is also considered in the paper. The method is applied to axisymmetric field problems. Numerical examples justifying the methods are presented.

Keywords: fundamental solution, potential field, measurement data, electromagnetic scattering, axisymmetric problems.

1. INTRODUCTION

Over the past decades, tremendous attention has been focused on the development of meshless methods which require neither domain nor boundary discretization. Among these methods, the MFS has emerged as an effective boundary-only meshless method for solving homogeneous equations. The MFS approximate solution satisfies identically the governing equations in the domain and, hence, only the satisfaction of the boundary conditions is required. Like other boundary methods, the MFS is applicable to any homogeneous elliptic boundary value problems, provided the fundamental solution of the governing equation is known. It has found extensive application in computing solution of a wide range of problems over the past three decades. The introduction of MFS is generally attributed to Kupradze and Aleksidze [1]. Recent development of the MFS for potential problems can be found in reviews [2, 3].

In application to the electromagnetic field calculation this technique is more known as the discrete sources method (DSM) [4–6] and consists in approximating the solution of the problem by a linear combination of discrete sources. These discrete sources are the fundamental solution of the differential equation of the problem. Note that there is a variety of methods which use “equivalent sources” for field expansion. The “equivalent sources” may be of any type as long as they are solutions of the wave equation. Therefore there are different names for similar concepts like the multiple multipole method (MMP) [7], the method of auxiliary sources (MAS) [8], the method of fictitious sources or Yasuura method [9] and the Generalized Multipole Technique (GMT) [10] etc. A review of these methods has been published in [11].

In this article we deal with some new electromagnetic applications MFS. The problems arising in the measurement of the external magnetic field of technical objects are considered in the first part of Section 2. We have an array \mathbf{H}_i of vectors of the magnetic field strength measured at the space points \mathbf{x}_i as initial data. The further measurement data processing assumes analytical or numerical transformations of this array: differentiation, integration, Fourier transformation, solution of differential equations etc. All the manipulations with the data array can be performed quite easily when \mathbf{x}_i is a regular set, e.g., when \mathbf{x}_i are placed in nodes of a rectangular mesh. In this case the data can be processed using standard numerical procedures based on the FE or FD technique. However, in many practical cases the measurement points \mathbf{x}_i are distributed in arbitrary way outside the boundary of the technical object and we get the problem of processing non-lattice scattered data. More over, often not all parts of the rounding space are accessible for measurement. For example, the measurement points \mathbf{x}_i can be placed in the top half space only. Our goal is to approximate the external magnetic field of the measured object using these scattered data. Such problems are considered in the first subsection.

In the second subsection we apply the MFS (or DSM) to 3D time-dependent problem of scattering of a short time electromagnetic pulse. This means that the problem can not be considered in the harmonic approximation $\sim e^{i\omega t}$. However, using the Laplace transform, one can get a sequence of time-harmonic problems and then apply the DSM.

In Section 3, we present a novel version of the MFS technique - the method of approximate fundamental solutions (MAFS) in applications to the field problems in domains with cylindrical symmetry. The results are compared with the analytic solution.

2. THE METHOD OF FUNDAMENTAL SOLUTIONS (MFS)

According to this technique an approximate solution of the BVP

$$L[u] = 0, \quad \mathbf{x} \in \Omega, \quad B[u] = g(\mathbf{x}), \quad \mathbf{x} \in \partial\Omega$$

is looked for in the form of the linear combination:

$$u(\mathbf{x}, \mathbf{q}) = \sum_{j=1}^N q_j \Psi(\mathbf{x} - \mathbf{y}_j). \quad (1)$$

Here the fundamental solution $\Psi(\mathbf{x} - \mathbf{y})$ satisfies exactly the homogeneous PDE except the singular (source) point \mathbf{y} but does not necessary satisfy boundary conditions. They are used to determine the unknowns q_j . The singular points \mathbf{y}_j are situated outside the solution domain. To get q_j we use the collocation of the boundary condition

$$\sum_{j=1}^N q_j B[\Psi(\mathbf{x}_i - \mathbf{y}_j)] = g(\mathbf{x}_i), \quad \mathbf{x}_i \in \partial\Omega, \quad i = 1, \dots, M \geq N. \quad (2)$$

We take the number of the collocation points M twice as large as the number of unknowns N and the resulting overdetermined linear system is solved by the procedure of the least squares.

2.1. MFS for problems of measurement data processing

The first task of measurement data processing is to present the data in compact form. This permits to predict the field outside the neighbourhood of the object. On the other hand this presentation can be used in the algorithm of identification of the field sources.

In order to compare the MFS with a traditional approach first consider the case when the data are measured on some surface Γ_{data} . Let us assume that this is a smooth closed surface which does

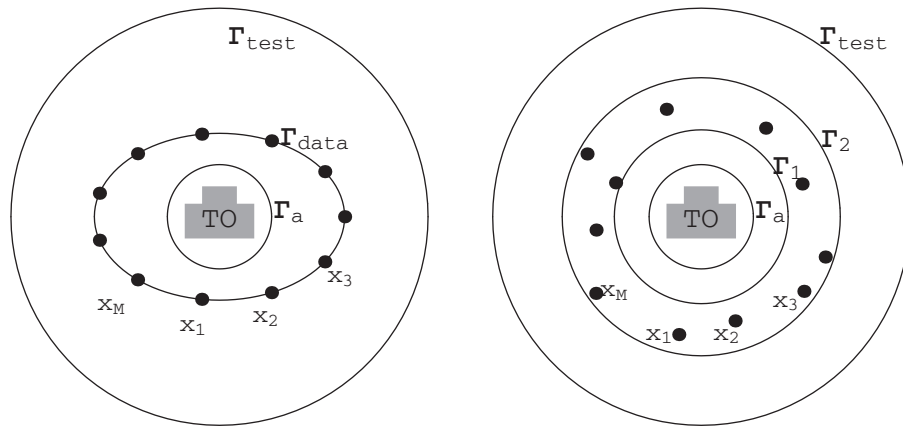


Fig. 1. The measurement data processing. The data are measured on the surface (left). The data are measured in the volume (right)

not intersect the boundary of the technical object (TO). So we can choose some closed auxiliary surface Γ_a between Γ_{data} and boundary of TO (see Fig. 1, left). The surface Γ_a contains all the sources of the TO under consideration and so, the field is potential outside of Γ_a . The measured value on Γ_{data} is the normal component of the magnetic field \mathbf{H}_n .

The boundary methods are classical tools for solving potential problems. The typical potential BVP related to the measurement described above can be formulated as follows. Let Ω be an unbounded region with a complement which is a simply connected region. Find $u(\mathbf{x})$ which satisfies the Laplace equation

$$\nabla^2 u(\mathbf{x}) = 0, \quad \mathbf{x} \in R^3 \setminus \Omega,$$

the Neumann boundary condition

$$\partial u(\mathbf{x}) / \partial \mathbf{n} = f(\mathbf{x}), \quad \mathbf{x} \in S \equiv \partial \Omega$$

and the growth condition $|u(\mathbf{x})| = O(|\mathbf{x}|)$, $|\mathbf{x}| \rightarrow \infty$. In this, \mathbf{n} is the inner unit normal to S directed into the bounded region associated with the surface $\partial \Omega$.

Using Green's representation formula, we obtain the integral equation

$$2\pi u(\mathbf{x}) + \int_S u(\mathbf{y}) \frac{\partial}{\partial \mathbf{n}_y} \left[|\mathbf{x} - \mathbf{y}|^{-1} \right] dS(\mathbf{y}) + (2\pi - \omega(\mathbf{x})) u(\mathbf{x}) = \int_S f(\mathbf{y}) |\mathbf{x} - \mathbf{y}|^{-1} dS(\mathbf{y}). \quad (3)$$

The quantity $\omega(\mathbf{x})$ is the solid interior angle at $\mathbf{x} \in S$.

This problem is well-studied, for both the cases of smooth boundaries and piecewise smooth boundaries. The method of solution includes:

1. a uniform triangulation of the surface S ,
2. the local approximation of the solution by piecewise polynomials,
3. collocation of the solution in the nodes,
4. approximation of the surface integrals in using a suitable quadrature,
5. solution of resulting linear system.

In [12] this technique is described with more details. To solve the integral equation (3) we use the code taken from the Prof. Kendall E. Atkinson home page:

<http://www.math.uiowa.edu/~atkinson/>

Example 1. Here we consider the magnetostatic problem when the field sources are located inside some bounded domain with a smooth enough boundary Γ_{data} . The field can be described by the potential $u(\mathbf{x})$:

$$\mathbf{H} = -\nabla u, \quad \nabla^2 u(\mathbf{x}) = 0, \quad \mathbf{x} \in \Omega.$$

The measured quantity of the problem is the normal component $\mathbf{H}_n = \partial u / \partial \mathbf{n} = f(\mathbf{x})$ on the surface Γ_{data} . So, we get the exterior Neumann problem described above. The data placed in Table 1 correspond to the solution of Eq. (3) when Γ_{data} is the ellipsoid with the semi-axes $a = 1$, $b = 1.5$, $c = 2$. The field sources are taken as a sum of the four dipoles with the potential:

$$u_{ex}(x) = \sum_{j=1}^4 d_j (\mathbf{x} - \xi_j, \mathbf{e}_j) \|\mathbf{x} - \xi_j\|^{-3},$$

where \mathbf{x} is an observation point, ξ_j are the coordinates of the dipole placement, \mathbf{e}_j is the direction of the dipole, and d_j is the value of the dipole moment. In particular, the following parameters are used in the calculations: $d_j = 1$, $\xi_1 = (0.1, 0, 0)$, $\xi_2 = (-0.1, 0, 0)$, $\xi_3 = (0, 0, 0.1)$, $\xi_4 = (0, 0, -0.1)$, $\mathbf{e}_1 = (1, 0, 0)$, $\mathbf{e}_2 = (-1, 0, 0)$, $\mathbf{e}_3 = (0, 0, 1)$, $\mathbf{e}_4 = (0, 0, -1)$.

Table 1. Example 1. The exterior Neumann problem

BIM			MFS			
N	e_{sq}	t_{cpu}	N	M	e_{sq}	t_{cpu}
18	$4_{10^{-3}}$	1.02	18	18	$3_{10^{-5}}$	0.0001
66	$6_{10^{-4}}$	14.9	66	66	$7_{10^{-8}}$	0.05
162	$1_{10^{-4}}$	57.1	66	162	$3_{10^{-9}}$	0.08
258	$9_{10^{-5}}$	114	162	258	$4_{10^{-11}}$	0.32
642	$1_{10^{-5}}$	301	258	642	$9_{10^{-15}}$	1.5

In the table we place the mean square root error

$$e_{\text{sq}} = \sqrt{\frac{1}{N} \sum_{j=1}^N [u(\mathbf{x}_j) - u_{ex}(\mathbf{x}_j)]^2},$$

where \mathbf{x}_j , $j = 1, \dots, N$ are the nodes which arise as a result of the triangulation of the surface Γ_{data} ; t_{cpu} is the time of the central processor in seconds.

The same problem was solved by the MFS. The approximate solution is looked for in the form:

$$u_N(\mathbf{x}) = \sum_{j=1}^N q_j \Psi(\mathbf{x} - \mathbf{y}_j), \quad \mathbf{y}_j \in \Gamma_a,$$

where

$$\Psi(\mathbf{x} - \mathbf{y}) = \frac{1}{\|\mathbf{x} - \mathbf{y}\|}$$

is the fundamental solution for 3D Laplacian.

The source points \mathbf{y}_j are distributed uniformly on the auxiliary surface Γ_a , which is placed inside the ellipsoid and contains all the field sources of $u(\mathbf{x})$ as it is depicted in Fig. 1 (right). We take the sphere with the radius $R_a = 0.15$ as the auxiliary surface Γ_a . We get the unknowns q_j as a result of the solution of the collocation system:

$$\sum_{j=1}^N q_j \frac{\partial}{\partial \mathbf{n}} \Psi(\mathbf{x}_i - \mathbf{y}_j) = f(\mathbf{x}_i), \quad \mathbf{x}_i \in \Gamma_{\text{data}}.$$

Here $i = 1, \dots, M \geq N$. The collocation points are taken at the same places as the nodes of the triangulation in the solution by the boundary integral method. To solve the overdetermined $M \times N$ system the procedure of the least squares is applied. In particular, we use the DLQRRV code from the Microsoft IMSL Libraries. We present the results of the solution in the left part of the table. The results show that MFS provides more precise data with the less CPU time.

In the problem of *Example 1* the measurement points \mathbf{x}_i are placed on some smooth surface Γ_{data} . However, in practice, the points \mathbf{x}_i are arbitrary placed in some vicinity of the TO.

Example 2. Without loss of generality we assume that the measurement points \mathbf{x}_i are distributed in the spherical layer between Γ_1 and Γ_2 with the radiuses R_1 and R_2 (see Fig. 1, right). While in *Example 1* only the normal component $\partial u(\mathbf{x})/\partial \mathbf{n}$ is approximated, here we should approximate the vector field $\mathbf{H}(\mathbf{x}_i)$. So, the collocation system takes the form

$$H_j(\mathbf{x}_i) = - \sum_{k=1}^N q_k \frac{\partial}{\partial x_j} \Psi(\mathbf{x}_i - \mathbf{y}_k), \quad j = 1, 2, 3, \quad i = 1, \dots, M.$$

Here

$$\frac{\partial}{\partial x_j} \Psi(\mathbf{x} - \mathbf{y}) = \frac{x_j - y_j}{|\mathbf{x} - \mathbf{y}|^3}.$$

The measurement (collocation) points $\mathbf{x}_i = (x_{i,1}, x_{i,2}, x_{i,3})$ are distributed in the spherical layer with the help of RNUF generator of pseudorandom numbers from the Microsoft IMSL Library:

$$\begin{aligned} x_{i,1} &= [R_1 + (R_2 - R_1) \zeta_i] \cos(\theta_i) \sin(\varphi_i), \\ x_{i,2} &= [R_1 + (R_2 - R_1) \zeta_i] \cos(\theta_i) \cos(\varphi_i), \\ x_{i,3} &= [R_1 + (R_2 - R_1) \zeta_i] \sin(\theta_i). \end{aligned} \quad (4)$$

Here $0 \leq \zeta_i \leq 1$, $-\pi/2 \leq \theta_i \leq \pi/2$, $0 \leq \varphi_i \leq 2\pi$ are pseudorandom values. The resulting $3M \times N$ linear system is solved by the procedure of the least squares. The data presented in Table 2 correspond to $R_1 = 1$, $R_2 = 1.5$.

Table 2. Example 2. Mean square root errors in approximation of the vector field in the spherical layer:
 $R_1 \leq r \leq R_2$

N	M	e_1	e_2	e_3
34	34	5.2×10^{-5}	5.3×10^{-5}	5.0×10^{-5}
66	66	2.6×10^{-9}	2.7×10^{-9}	2.6×10^{-9}
162	162	2.3×10^{-12}	2.1×10^{-12}	2.2×10^{-12}
258	258	7.7×10^{-16}	7.8×10^{-16}	7.1×10^{-16}

The absolute errors are computed for each component of the field

$$e_j = \sqrt{\frac{1}{N_t} \left[H_j(\mathbf{x}_{t,i}) + \sum_{k=1}^N q_k \frac{\partial}{\partial x_j} \Psi(\mathbf{x}_{t,i} - \mathbf{y}_k) \right]^2}, \quad j = 1, 2, 3.$$

Here the test points $\mathbf{x}_{t,i}$ are placed on the sphere Γ_{test} with the radius $R_t = 3$. We take $N_t = 500$ test points in all the calculations. The errors decrease very fast with the growth of N and for $N = 258$ they are close to the precision error.

Example 3. Let us assume that the magnetic field can be measured in the upper subspace $x_3 \geq 0$ only. We calculate the coordinates of the measurement points using the same formulae (4)

Table 3. Example 3. Mean square root errors in approximation of the vector field in the half of the spherical layer: $R_1 \leq r \leq R_2$, $x_3 \geq 0$

N	M	e_1	e_2	e_3
34	34	3.6×10^{-4}	2.6×10^{-4}	3.4×10^{-4}
66	66	1.5×10^{-7}	1.2×10^{-7}	1.5×10^{-7}
162	162	1.6×10^{-10}	1.3×10^{-10}	1.8×10^{-10}
258	258	4.1×10^{-13}	4.9×10^{-13}	5.2×10^{-13}

with $0 \leq \theta_i \leq \pi/2$. The number of the measurement points M we leave the same. The results are placed in Table 3. The test points $\mathbf{x}_{i,i}$ are the same as in *Example 2*. The errors increase from 100 to 1000 times but still are very small. So, the vector field $\mathbf{H}(\mathbf{x})$ is reconstructed with a high precision.

In Table 4 the errors in approximation of the vector field $\mathbf{H}(\mathbf{x})$ using the data from the part of the spherical layer $0 \leq \theta_i \leq \pi/4$. The errors increase, but the exactness of the field reconstruction is still high for $N = 258$.

Table 4. Example 3. Mean square root errors in approximation of the vector field in the part of the spherical layer: $R_1 \leq r \leq R_2$, $0 \leq \theta_i \leq \pi/4$

N	M	e_1	e_2	e_3
34	34	5.0×10^{-4}	5.1×10^{-4}	4.8×10^{-4}
66	66	3.5×10^{-7}	3.8×10^{-7}	4.3×10^{-7}
162	162	1.3×10^{-9}	1.1×10^{-9}	1.1×10^{-9}
258	258	6.0×10^{-11}	6.9×10^{-11}	7.5×10^{-11}

2.2. MFS for problems of electromagnetic scattering

Over the past several years, many modelling techniques have been proposed to solve the Maxwell system

$$\varepsilon_a \frac{\partial \mathbf{E}}{\partial t} + \alpha \mathbf{E} = \text{rot } \mathbf{H}, \quad (5)$$

$$\mu_a \frac{\partial \mathbf{H}}{\partial t} = -\text{rot } \mathbf{E}, \quad (6)$$

It is written in dimensionless form (see Appendix).

The finite-difference-time-domain (FDTD) method so extensively used for computing electromagnetic scattering problems [13], suffers from the requirement to provide the absorbing of outgoing waves on the outer surface of the solution domain without reflections.

This problem one can overcome applying the MFS technique together with the Laplace transform:

$$f \rightarrow \hat{f}(s) = \int_0^\infty e^{-st} f(t) dt.$$

Note that the combination of the MFS and Laplace's transform first was proposed in [15]. As a result of applying this transform to Maxwell's system (5), (6) we get the following system:

$$\varepsilon_a s \hat{\mathbf{E}}(s) + \alpha \hat{\mathbf{E}}(s) = \text{rot } \hat{\mathbf{H}}(s), \quad \mu_a s \hat{\mathbf{H}}(s) = \text{rot } \hat{\mathbf{E}}(s).$$

Denoting $\varepsilon_a s + \alpha = ik_0 \hat{\varepsilon}_a(s)$, $\mu_a s = ik_0 \hat{\mu}_a(s)$, we obtain the system

$$\text{rot } \hat{\mathbf{H}}(s) = ik_0 \hat{\varepsilon}_a(s) \hat{\mathbf{E}}(s), \quad \text{rot } \hat{\mathbf{E}}(s) = -ik_0 \hat{\mu}_a(s) \hat{\mathbf{H}}(s) \quad (7)$$

which formally can be regarded as a problem in a frequency domain with the electromagnetic properties $\dot{\epsilon}_a(s)$, $\dot{\mu}_a(s)$ and with the wave number k_0 (A.7), [14]. So, we can apply the DSM technique [4–6] to approximate the field $\{\hat{\mathbf{E}}(s), \hat{\mathbf{H}}(s)\}$ with each fixed s .

For system (7) the DSN approach is as follows. Let $\{\hat{\mathbf{e}}(s, \|\mathbf{r} - \mathbf{a}\|, \mathbf{p}), \hat{\mathbf{h}}(s, \|\mathbf{r} - \mathbf{a}\|, \mathbf{p})\}$ be field of a dipole \mathbf{p} placed at $\mathbf{r} = \mathbf{a}$. We can write this field using Hertz's vector $\hat{\mathbf{\Pi}}$

$$\hat{\mathbf{e}} = [k_0 \dot{\epsilon}_a(s)]^{-1} \text{rot rot } \hat{\mathbf{\Pi}}, \quad \hat{\mathbf{h}} = i \text{rot } \hat{\mathbf{\Pi}},$$

where

$$\hat{\mathbf{\Pi}} = \Psi(\|\mathbf{r} - \mathbf{a}\|, s) \mathbf{p},$$

\mathbf{p} is an arbitrary constant vector and Ψ is a scalar function of $\|\mathbf{r} - \mathbf{a}\|$. It is easy to show that the pair $\{\hat{\mathbf{e}}, \hat{\mathbf{h}}\}$ satisfies (7) when $\Psi(s, \|\mathbf{r} - \mathbf{a}\|)$ is a solution of the equation:

$$\nabla^2 \Psi - k_0^2 \dot{\epsilon}_a(s) \dot{\mu}_a(s) \Psi = 0.$$

We use the fundamental solution

$$\Psi(\|\mathbf{r} - \mathbf{a}\|, s) = \exp\left(-\sqrt{k_0^2 \dot{\epsilon}_a(s) \dot{\mu}_a(s)} \|\mathbf{r} - \mathbf{a}\|\right) \|\mathbf{r} - \mathbf{a}\|^{-1}$$

and so, the field $\{\hat{\mathbf{e}}(s, \|\mathbf{r} - \mathbf{a}\|, \mathbf{p}), \hat{\mathbf{h}}(s, \|\mathbf{r} - \mathbf{a}\|, \mathbf{p})\}$ satisfies (7) when $\mathbf{r} \neq \mathbf{a}$. We choose the branch of the square root in the way that provides the condition:

$$\lim_{s \rightarrow \infty} \Psi(\|\mathbf{r} - \mathbf{a}\|, s) = 0$$

as it should be for any Laplace transform.

Applying the MFS, we approximate a solution of (7) by the linear combinations of the elementary fields:

$$\hat{\mathbf{E}}(s, \mathbf{r}) = \sum_{k=1}^N \hat{\mathbf{e}}(s, \|\mathbf{r} - \mathbf{a}_k\|, \mathbf{p}_k), \quad \hat{\mathbf{H}}(s, \mathbf{r}) = \sum_{k=1}^N \hat{\mathbf{h}}(s, \|\mathbf{r} - \mathbf{a}_k\|, \mathbf{p}_k). \quad (8)$$

Here the singular points \mathbf{a}_k are placed outside the solution domain and the free parameters \mathbf{p}_k should be found from the boundary conditions. When the scattering from a perfectly conducting body Ω is considered these conditions on the boundary $\partial\Omega$ can be written as follows $\mathbf{E}_\tau^0 = \mathbf{E}_\tau + \mathbf{E}_\tau^{(inc)} = 0$, $\mathbf{H}_\tau^0 = \mathbf{H}_\tau + \mathbf{H}_\tau^{(inc)} = 0$, where $\{\mathbf{E}^{(inc)}, \mathbf{H}^{(inc)}\}$ is a known incident of the electromagnetic source; $\{\mathbf{E}, \mathbf{H}\}$ is a scattered field; τ is the tangent unit vector to $\partial\Omega$. So, the Laplace transforms satisfy the same conditions

$$\hat{\mathbf{E}}_\tau(s, \mathbf{r}) = -\hat{\mathbf{E}}_\tau^{(inc)}(s, \mathbf{r}), \quad \hat{\mathbf{H}}_\tau(s, \mathbf{r}) = -\hat{\mathbf{H}}_\tau^{(inc)}(s, \mathbf{r}), \quad \mathbf{r} \in \partial\Omega. \quad (9)$$

The rest part of the algorithm is the same as the one described in the previous subsection. We choose the collocation points $\mathbf{r}_i \in \partial\Omega$ and write conditions (9). As a result we get a linear system for free parameters \mathbf{p}_k which is solved by the standard procedure.

The main difficulty in this way is inversion of the Laplace transform, i.e. for given $F(s)$ to find $f(t)$. There are a lot of numerical techniques available to invert Laplace transforms. In this work we use two procedures. The first one is a straightforward application of a numerical integration procedure to evaluate Bromwich's integral [16]. The second method of inversion suggested by Week [17] is based upon expressing the numerical inversion in the term of Laguerre polynomials:

$$f(t) = e^{at} \sum_{m=0}^M a_m e^{-bt/2} L_m(bt).$$

As a result, for each particular value s_m we can compute the Laplace transform $F(s_m)$ of a time-dependent value $f(t)$ which should be determined. For example, it can be a component of the scattered field at some point of the interest or it can be an integral characteristic of the scattering body. Then the data $\{s_m, F(s_m)\}$ are used in the procedure of the inversion of the Laplace transform. Note that the set $\{s_m\}$ depends on the method of inversion used. As a result we get $\tilde{f}(t)$ which approximates $f(t)$.

Example 4. To test the method we have computed a non-stationary electromagnetic field scattered by a conducting sphere. The source of the incident field is a Hertzian dipole placed apart of the sphere.

A dipole source located in a free space at \mathbf{r}_s directed along \mathbf{e}_z creates the electric field [18]:

$$\mathbf{E}_d(\mathbf{r} - \mathbf{r}_s, t) = \frac{1}{4\pi\epsilon_0} \left\{ \frac{\left[\dot{f}(t-r) + \frac{f(t-r)}{r} \right]}{r^2} \begin{pmatrix} 3\frac{(z-z_s)(x-x_s)}{r^2} \\ 3\frac{(z-z_s)(y-y_s)}{r^2} \\ 3\frac{(z-z_s)^2}{r^2} - 1 \end{pmatrix} + \frac{\ddot{f}(t-r)}{r} \begin{pmatrix} \frac{(z-z_s)(x-x_s)}{r^2} \\ \frac{(z-z_s)(y-y_s)}{r^2} \\ \frac{(z-z_s)^2}{r^2} - 1 \end{pmatrix} \right\}. \quad (10)$$

The magnetic field of this dipole is:

$$\mathbf{H}_d(\mathbf{r} - \mathbf{r}_s, t) = \frac{1}{4\pi\epsilon_0 r^2} \left[\ddot{f}(t-r) + \frac{\dot{f}(t-r)}{r} \right] \begin{pmatrix} -(y-y_s) \\ (x-x_s) \\ 0 \end{pmatrix}. \quad (11)$$

The time dependence we take in the form of a well-known pulse function [18]:

$$f(t) = \begin{cases} 10 - 15 \cos(\omega_1 t) + 6 \cos(\omega_2 t) - \cos(\omega_3 t), & t < \tau, \\ 0, & t > \tau, \end{cases} \quad (12)$$

where

$$\omega_n = \frac{2\pi n}{\tau}, \quad \tau = 1 \text{ ns}.$$

From definition (12) it is easy to get explicit expressions for $\dot{f}(t)$ and $\ddot{f}(t)$.

The Laplace transforms $L[f(t)]$, $L[\dot{f}(t)]$ and $L[\ddot{f}(t)]$ are given by:

$$L[f(t)] = 10\hat{\Phi}_c(s|\omega_0) - 15\hat{\Phi}_c(s|\omega_1) + 6\hat{\Phi}_c(s|\omega_2) - \hat{\Phi}_c(s|\omega_3),$$

$$L[\dot{f}(t)] = 15\omega_1\hat{\Phi}_s(s|\omega_1) - 6\omega_2\hat{\Phi}_s(s|\omega_2) + \omega_3\hat{\Phi}_s(s|\omega_3),$$

$$L[\ddot{f}(t)] = 15\omega_1^2\hat{\Phi}_c(s|\omega_1) - 6\omega_2^2\hat{\Phi}_c(s|\omega_2) + \omega_3^2\hat{\Phi}_c(s|\omega_3),$$

where

$$\hat{\Phi}_c(s|\omega) = \frac{s(1 - e^{-s\tau})}{\omega^2 + s^2}, \quad \hat{\Phi}_s(s|\omega) = \frac{\omega(1 - e^{-s\tau})}{\omega^2 + s^2},$$

and we apply the well-known formula

$$L[f(t-r)] = e^{-rs}L[f(t)]$$

In Fig. 2 we show the data concern to the scattering problem. The dipole source (10), (11) is located at the point $(0, 0, 1)$. The observation point is $(1, 0, 0)$. The duration of the impulse is equal to 1 ns. The scattering body is a conducting sphere at the radius $r_s = 0.2$ placed at the point $(0, 0, 0)$, i.e, we calculate in $(1, 0, 0)$ the field reflected by the conducting sphere placed at

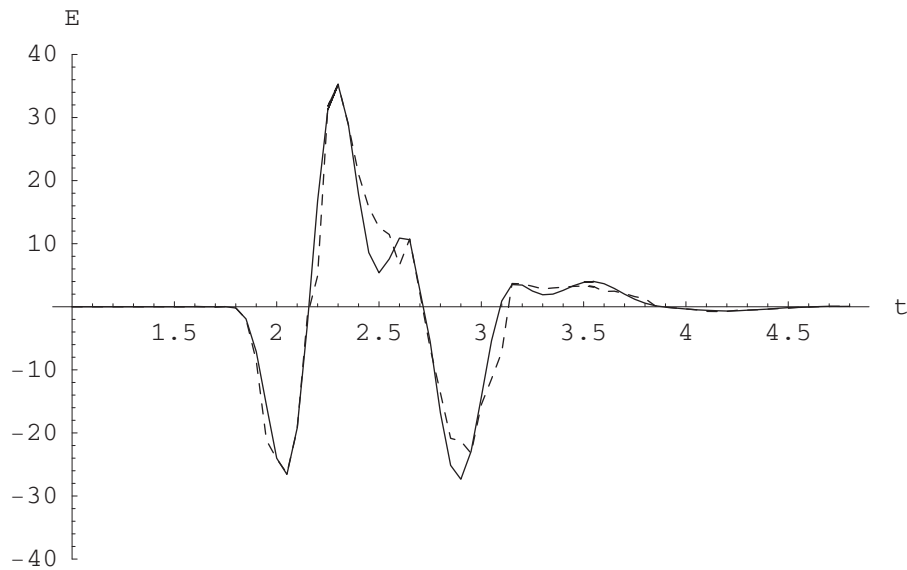


Fig. 2. Two methods of the Laplace inversion

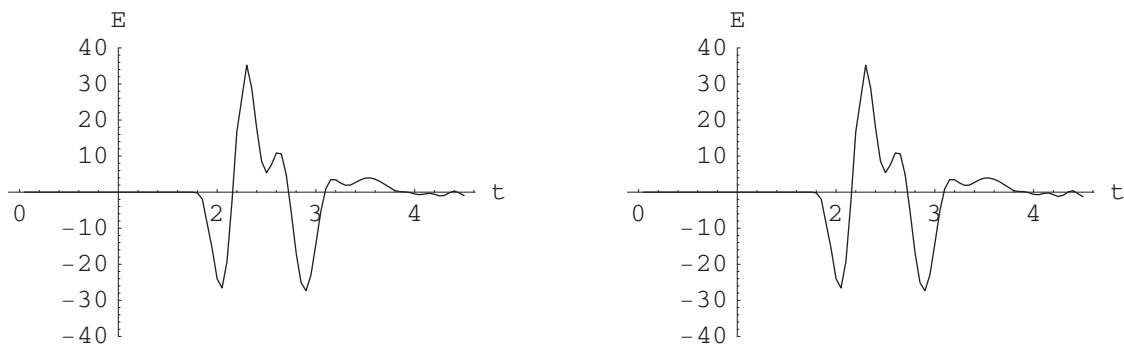


Fig. 3. Calculation of the scattered field with different number of the basis functions ($N = 48$ – left, and $N = 70$ – right)

$(0, 0, 0)$. We use 16 sources placed inside the scatterer to model the scattered field (8). The number of collocation points on the sphere is equal to 48. We compare two different methods of inversion: algorithm [16] with the direct evaluation of Bromwich's integral (the dashed line) and the Weeks' algorithm [17] (the solid line). It should be stressed that the methods use different approaches and they use different data $\{s_m, F(s_m)\}$ for inverting procedures. One can see a good agreement of the important characteristics of the impulse as: (a) beginning of the signal, (b) the location of the maximal amplitude of the scattered wave, (c) the value of the maximum of the wave, (d) the end of the signal.

In Fig. 3 the data corresponding to the different number of the free parameters ($N = 48$ – left, and $N = 70$ – right) are presented. The number of the collocation points is the same. One can see a good agreement between the calculations. This indicates a high precision of the numerical result.

3. THE METHOD OF APPROXIMATE FUNDAMENTAL SOLUTIONS

One of the main restrictions of using boundary methods is that they can be applied only in cases when there exists a representative set of known exact solutions of PDEs under consideration. In this section we describe the numerical technique which is based on the use of *approximate* fundamental solutions of PDEs and it makes it possible to extend the field of application of the boundary methods

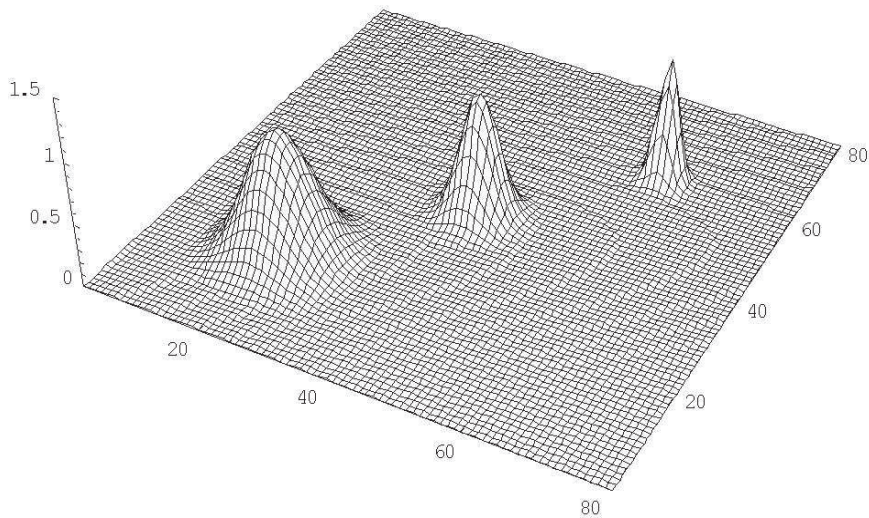


Fig. 4. The functions $I_{30,9}^{(1)}(\mathbf{x}, \xi)$, $I_{50,14}^{(1)}(\mathbf{x}, \xi)$, and $I_{100,18}^{(1)}(\mathbf{x}, \xi)$ centered at $(-0.25, -0.25)$, $(0, 0)$, and $(0.25, 0.25)$, respectively

to the problems where exact solutions can't be found or are very complex [19–21]. This technique uses a new kind of the δ -shaped basis functions in the form of the truncated series

$$I_{M,\chi}(x, \xi) = \sum_{n=1}^M c_n(\xi) \varphi_n(x)$$

over some orthogonal system φ_n . These functions essentially differ from zero only inside some neighborhood of the center point ξ (Fig. 4). From this point of view they are similar to the compactly supported radial basis functions (CS-RBF) [22]. The algorithm of construction of the coefficients $c_n(\xi)$ is given in [20, 21]. Using the MAFS technique to solve the PDE $L[w] = 0$ we take the eigenfunctions $\varphi_{\mathbf{n}}(x)$ of the differential operator $L[\dots]$. And the approximate fundamental solutions $\Psi(x, \xi)$ are obtained as solutions of the PDE with $I_{M,\chi}(x, \xi)$ source functions in the right hand side

$$L[\Psi] = I_{M,\chi}(x, \xi).$$

Since $\varphi_{\mathbf{n}}(\mathbf{x})$ satisfy

$$L[\varphi_{\mathbf{n}}] = \lambda_n \varphi_{\mathbf{n}},$$

the functions Ψ can be found in the explicit analytic form:

$$\Psi(x, \xi) = \sum_{n=1}^M (c_{\mathbf{n}}(\xi)/\lambda_n) \varphi_{\mathbf{n}}(x).$$

The rest part of the MAFS approach is the same as in the MFS. An approximate solution is looked for in the form of the linear combination like (1). The unknowns q_n are obtained by the collocation of the boundary conditions.

Example 5. Here we illustrate this technique in application to the BVP in an infinite domain [21]. Let us consider the sphere with the radius $R_s < 1$ placed between two infinite planes $z = \pm 1$. The Laplace equation written in the polar coordinates has the form:

$$\frac{1}{r} \frac{\partial}{\partial r} \left(r \frac{\partial w}{\partial r} \right) + \frac{\partial^2 w}{\partial z^2} = 0.$$

Placing the center of the sphere at the origin $(0, 0)$ and setting potential of the planes equal to zero, we get the boundary conditions:

$$w(r, z = 1) = \frac{\partial w}{\partial z}(r, z = 0) = 0.$$

So, the orthogonal system $\varphi_n(z) = \cos(n - 1/2)\pi z$ can be used to construct the δ -shaped functions

$$I_{M,\chi}(z, \xi) = \sum_{n=1}^M c_n(\eta) \cos(n - 1/2)\pi z. \quad (13)$$

We take the MAFS basis functions as solutions of the PDE:

$$\frac{1}{r} \frac{\partial}{\partial r} \left(r \frac{\partial \Psi}{\partial r} \right) + \frac{\partial^2 \Psi}{\partial z^2} = \delta(r - \xi) \sum_{n=1}^M c_n(\eta) \cos\left(n - \frac{1}{2}\right)\pi z. \quad (14)$$

Note that applying the MFS approach one should take the right hand side of (14) in the form $\delta(r - \xi) \delta(z - \eta)$. However, we replace $\delta(z - \eta)$ by its approximation (13).

Looking for a solution in the form

$$\Psi(r, z; \xi, \eta) = \sum_{n=1}^M \Phi_n(r, \xi) c_n(\eta) \cos(n - 1/2)\pi z, \quad (15)$$

one obtains the following equation for each Φ_n :

$$\frac{1}{r} \frac{d}{dr} \left(r \frac{d}{dr} \Phi_n \right) - \mu_n^2 \Phi_n = \delta(r - \xi).$$

Up to a constant factor, the solution is:

$$\Phi_n(r, \xi) = \begin{cases} I_0(\mu_n r) K_0(\mu_n \xi), & r \leq \xi, \\ K_0(\mu_n r) I_0(\mu_n \xi), & r > \xi. \end{cases} \quad (16)$$

Table 5. Sphere with the radius R_s between two planes. Capacity with different R_s

R_s	0.2	0.25	0.3	0.35	0.4	0.5
present	1.46	1.91	2.40	2.94	3.54	4.98
[23]	1.46	1.90	2.38	2.90	3.47	4.78

In Table 5, we place the capacity $C = Q/U$ of the system. Here Q is the total charge of the sphere

$$Q = \varepsilon_0 \int \frac{\partial w}{\partial n} ds$$

and U is the difference of the potential between the sphere and planes. The results are compared with the ones obtained in [23]:

$$C/R_s = 1 + \sigma + \sigma^2 + \sigma^3 + \sigma^4 + o(R_s) \quad (17)$$

where $\sigma = (R_s/R_c) \ln 2$. The difference between the two data increase with the growth of R_s . This can be explained by the growth of the remainder term in (17). More detailed description of this technique is in [21]. In [14, 24, 25] the MAFS technique was applied to the problem of scattering of plane electromagnetic waves from penetrable inhomogeneous bodies. Recent development of the MAFS basis functions are given in [26, 27].

4. CONCLUDING REMARKS

The MFS and its modification MAFS can be regarded as a convenient tool for electromagnetic calculations. We demonstrate it in application to problems of measurement data processing. This technique allows to reconstruct the vector field $\mathbf{H}(\mathbf{x})$ in the whole space outside the auxiliary surface Γ_a using the scattered data from the part of the layer between the surfaces Γ_1, Γ_2 . Note that in this paper we describe the algorithm which can handle exact values of the measured data. We intend to take into account the measurement errors in further study.

Combination of the MFS and Laplace transform gets an effective algorithm for time-dependent problems. It can be extended to problems with penetrable scatterer and to problems with a few scatterers. Note that the problems with a few scatterers are quite difficult for the FTTD technique.

The MAFS technique which is based on the use of approximate fundamental solutions extends the field of application of the boundary methods to the problems where exact solutions can't be found or are very complex.

APPENDIX

The Maxwell system in a homogeneous dielectric medium is

$$\varepsilon_0 \varepsilon_a \frac{\partial \mathbf{E}}{\partial t} + \sigma \mathbf{E} = \text{rot } \mathbf{H}, \quad (\text{A.1})$$

$$\mu_0 \mu_a \frac{\partial \mathbf{H}}{\partial t} = -\text{rot } \mathbf{E}, \quad (\text{A.2})$$

where $\{\mathbf{E}(t, \mathbf{r}), \mathbf{H}(t, \mathbf{r})\}$ are the vectors of electrical and magnetic field correspondingly; ε_a and μ_a are the relative permittivity and permeability; ε_0 and μ_0 are the permittivity and permeability of the free space; σ is the conductivity of a scattered body. Transform the system to the dimensionless form using some basis scaling values T, L, E_m, H_m :

$$\mathbf{E}^* = \mathbf{E}/E_m, \quad \mathbf{H}^* = \mathbf{H}/H_m, \quad \mathbf{r}^* = \mathbf{r}/L, \quad t^* = t/T. \quad (\text{A.3})$$

We assume that the scaling values E_m, H_m, L, T satisfy the conditions:

$$\frac{L}{T} = \frac{1}{\sqrt{\varepsilon_0 \mu_0}} = c, \quad \frac{E_m}{H_m} = \sqrt{\frac{\mu_0}{\varepsilon_0}}, \quad \alpha = \sigma T / \varepsilon_0. \quad (\text{A.4})$$

After these transforms we get the dimensionless system:

$$\varepsilon_a \frac{\partial \mathbf{E}}{\partial t} + \alpha \mathbf{E} = \text{rot } \mathbf{H}, \quad (\text{A.5})$$

$$\mu_a \frac{\partial \mathbf{H}}{\partial t} = -\text{rot } \mathbf{E} \quad (\text{A.6})$$

Consider the Maxwell system (A.1), (A.2) in a nonconducting medium ($\sigma = 0$). Considering the harmonic time-dependence $\sim e^{i\omega t}$, one gets the system

$$i\omega \varepsilon_0 \varepsilon_a \mathbf{E} = \text{rot } \mathbf{H}, \quad i\omega \mu_0 \mu_a \mathbf{H} = -\text{rot } \mathbf{E}.$$

Using (A.4) one gets the dimensionless system

$$i\omega L \sqrt{\varepsilon_0 \mu_0} \varepsilon_a \mathbf{E} = \text{rot } \mathbf{H}, \quad i\omega L \sqrt{\varepsilon_0 \mu_0} \mu_a \mathbf{H} = -\text{rot } \mathbf{E}.$$

Denoting $k_0 = \omega L \sqrt{\varepsilon_0 \mu_0}$ finally get

$$ik_0 \varepsilon_a \mathbf{E} = \text{rot } \mathbf{H}, \quad ik_0 \mu_a \mathbf{H} = -\text{rot } \mathbf{E}. \quad (\text{A.7})$$

REFERENCES

- [1] V.D. Kupradze, M.A. Aleksidze. The method of functional equations for the approximate solution of certain boundary value problems. *USSR Comput Math Math Phys.*, **4**(4): 82–126, 1964.
- [2] G. Fairweather and A. Karageorghis. The method of fundamental solutions for elliptic boundary value problems. *Advances in Comp. Math.*, **9**: 69–95, 1998.
- [3] M.A. Golberg and C.S. Chen, The Method of Fundamental Solutions for Potential, Helmholtz and Diffusion Problems. In: M.A. Golberg, eds., *Boundary Inetgral Methods – Numerical and Mathematical Aspects*, pp. 103–176. Computational Mechanics Publications, 1998.
- [4] A. Doicu, Y. Eremin, T. Wriedt. *Acoustic and Electromagnetic Scattering Analysis using Discrete Sources*. Academic Press, San Diego, 2000.
- [5] Y.A. Eremin, A.G. Sveshnikov. A computer technology for the discrete source method in scattering problems. *Comput Math Modeling*, **14**(1): 16–25, 2003.
- [6] A., Doicu, T. Wriedt, Y. Eremin. *Light scattering by systems of particles. Null-field method with discrete sources – theory and programs*. Springer, Berlin, Heidelberg, New York, 2006.
- [7] Ch. Hafner, L. Bomholt. *The 3D electromagnetic wave simulator, 3D MMP software and user’s guide*. Wiley, Chichester, 1993.
- [8] D.I. Kaklamani, H.T. Anastassiou. Aspects of the method of auxiliary sources in computational electromagnetics. *IEEE Antennas Propag Mag*, **44**(3): 48–64, 2002.
- [9] M. Kawano, H. Ikuno, M. Nishimoto. Numerical analysis of 3-D scattering problems using the Yasuura method. *IEICE Trans Electron.*, **1E79-C**: 1358–63, 1996.
- [10] A.C. Ludwig. The generalized multipole technique. *Comput Phys Commun.*, **68**: 306–14, 1991.
- [11] G. Fairweather, A. Karageorghis, P.A. Martin. The method of fundamental solutions for scattering and radiation problems. *Engineering Analysis with Boundary Elements*, **27**: 759–769, 2003.
- [12] K. Atkinson., A survey of boundary integral equation method for the numerical solution of Laplace’s equation in three dimension. In: M. Golberg, eds., *Numerical Solution of Integral Equations*, pp. 1–34. Plenum Press, New York, 1990.
- [13] A. Taflove. *Computational Electrodynamics – The Finite-Difference Time-Domain Method*. Artech House, Boston, 1995.
- [14] S.Y. Reutskiy. Trefftz type method for 2D problems of electromagnetic scattering from inhomogeneous bodies. *Computer Assisted Mechanics and Engineering Sciences*, **10**: 609–618, 2003.
- [15] C.S. Chen, M.A. Golberg, Y.F. Rashed. A mesh free method for linear diffusion equations. *Numerical Heat Transfer, Part B*, **33**: 469–486, 1998.
- [16] R. Piessens, R. Huismans. Algorithm 619: automatic numerical inversion of the Laplace transform. *ACM Trans. Math. Softw.*, **10**: 348–356, 1984.
- [17] B.S. Garbow, G. Guinta, J.N. Lyness. Algorithm 662: A FORTRAN software package for the numerical inversion of the Laplace transform basedon Weeks’ method. *ACM Trans. Math. Softw.*, **14**: 163–175, 1988.
- [18] De Moerloose J., De Zutter D. Surface integral representation radiation boundary condition for the FDTD method. *IEEE Trans. Antennas and Propagation*, **41**: 890–898, 1993.
- [19] S.Y. Reutskiy. A boundary method of Trefftz type with approximate trial functions. *Engineering Analysis with Boundary Elements*, **26**: 341–353, 2002.
- [20] S.Y. Reutskiy. A boundary method of Trefftz type for PDEs with scattered data. *Engineering Analysis with Boundary Elements*, **29**: 713–724, 2005.
- [21] S.Y. Reutskiy. The method of approximate fundamental solutions for axisymmetric problems with Laplace operator. *Engineering Analysis with Boundary Elements*, **31**: 410–415, 2007.
- [22] C.S. Chen, M.A. Golberg, R.S. Schaback. Recent developments of the dual reciprocity method using compactly supported radial basis functions. In: Y.F. Rashed, ed., *Transformation of Domain Effects to the Boundary*. WIT Press, Boston, 2002.
- [23] W.D. Collins. On the solution of some axisymmetric boundary value problems by means of integral equations. IV. The electrostatic potential due to a spherical gap between two infinite conducting planes. *Proc. Edin. Math. Soc.*, **12**: 95–106, 1960.
- [24] S. Reutskiy, B. Tirozzi. A new boundary method for electromagnetic scattering from inhomogeneous bodies, *Journal of Quantative Spectroscopy & Radiative Transfer*, **72**: 837–852, 2002.
- [25] S.Y. Reutskiy and B. Tirozzi. A new boundary method for electromagnetic scattering from inhomogeneous bodies: H-polarized waves. *Journal of Quantative Spectroscopy & Radiative Transfer*, **83**: 313–320, 2004.
- [26] H. Y. Tian, S. Reutskiy, C. S. Chen. A basis function for approximation and the solutions of partial differential equations. *Numerical Methods for Partial Differential Equations*, **24**: 1018–1036, 2008.
- [27] S. Yu. Reutskiy, C. S. Chen, H. Y. Tian. A boundary meshless method using Chebyshev interpolation and trigonometric basis function for solving heat conduction problems, *International Journal for Numerical Methods in Engineering*, **74**: 1519–1644, 2008.